 Communications in Theoretical Physics

Commun. Theor. Phys. **73** (2021) 095005 (8pp) https://doi.org/10.1088/1572-9494/ac0a65

Significance of Stefan blowing effect on flow and heat transfer of Casson nanofluid over a moving thin needle

A M Jyothi[1], R Naveen Kumar[2], R J Punith Gowda[2] and B C Prasannakumara[2]

[1] Bangalore Institute of Technology, Bangalore, India
[2] Department of Studies and Research in Mathematics, Davangere University, Davangere-577002, Karnataka, India

E-mail: dr.bcprasanna@gmail.com

Received 1 January 2021, revised 9 June 2021
Accepted for publication 11 June 2021
Published 5 August 2021

Abstract

The current mathematical model explains the influence of non-linear thermal radiation on the Casson liquid flow over a moving thin needle by considering Buongiorno's nanofluid model. The influences of Stefan blowing, Dufour and Soret effects are also considered in the model. The equations which represent the described flow pattern are reduced to ordinary differential equations (ODEs) by using apt similarity transformations and then they are numerically solved with Runge–Kutta-Fehlberg's fourth fifth-order method (RKF-45) with shooting process. The impacts of pertinent parameters on thermal, mass and velocity curves are deliberated graphically. Skin friction, rate of heat and mass transfer are also discussed graphically. Results reveal that, the increase in values of Brownian motion, thermophoresis, Dufour number, heating and radiative parameters improves the heat transfer. The increasing values of the Schmidt number deteriorates the mass transfer but a converse trend is seen for increasing values of the Soret number. Finally, the escalating values of the radiative parameter decays the rate of heat transfer.

Keywords: moving thin needle, Brownian motion and thermophoretic diffusion, non-linear thermal radiation, Stefan blowing condition

(Some figures may appear in colour only in the online journal)

Nomenclature

$R(x)$	Shape of thin needle
ψ	Stream function
C_f	Skin friction coefficient
$f(\eta)$	Velocity profile
k	Thermal conductivity
Re_x	Local Reynolds number
D_B	Brownian diffusion coefficient
N_r	Radiative parameter
ν	Kinematic viscosity
Pr	Prandtl number
(x, r)	Directions
(u, v)	Components of Velocity
D_T	Thermophoretic diffusion co-efficient
α	Thermal diffusivity
ρ	Density of base fluid
μ	Dynamic viscosity
(ρC_p)	Heat capacitance
T	Fluid temperature
C	Fluid concentration
Du	Dufour number
T_m	Fluid mean temperature

D_m	Mass diffusivity coefficient
C_s	Nanoparticle concentration susceptibility
k^*	mean absorption coefficient
N_b	Brownian motion parameter
N_t	thermophoresis parameter
θ_r	heating parameter
Sc	Schmidt number
s	Stefan blowing parameter
λ	Velocity ratio parameter
β^*	Casson parameter
Nu	Nusselt number
Sh_x	Sherwood number
σ^*	Stefan-Boltzman constant
T_w	Surface temperature
T_∞	Ambient temperature
C_w	Surface concentration
C_∞	Ambient concentration
$U = U_w + U_\infty$	Composite velocity
$\theta(\eta)$	Temperature profile
τ	Ratio of effective heat capacity
c	Needle thickness size
Sr	Soret number
K_T	Thermal diffusion ratio
C_p	Particular heat at uniform pressure
$\chi(\eta)$	Concentration profile

1. Introduction

The boundary layer stream with thin needles has extensive applications in biomedical and engineering fields. For example, it is generally used in a protected thermocouple to calculate wind velocity, hot wire anemometer, wire coating and circulatory problems. Recently, Mabood *et al* [1] examined the consequences of chemically reacting cross stream of non-Newtonian fluid through a thin moving needle. Souayeh *et al* [2] deliberated the non-linear thermal radiation impact on the Casson liquid flow through a needle with thermophoresis and Brownian motion. Ramesh *et al* [3] examined the hybrid nanoliquid flow through a needle. Xiong *et al* [4] illustrated the dissipative flow of cross nanofluid past an upright thin needle. Kumar *et al* [5] deliberated the particle deposition on the Casson liquid flow past a thin moving needle.

Due to an increase in industrial and technological uses in recent years, the non-Newtonian liquid flow is attracting the attention of more researchers. For example, if a person uses non-Newtonian liquids as coolers or heat exchangers, the required suction capacity can be greatly reduced. The characteristics of non-Newtonian liquids are different from those of the viscous liquid. Non-Newtonian liquid levels are relatively uneven and more complex compared to Newtonian liquids. In the literature, it is sometimes said that in many aspects, the Casson model is better than that of the standard visco-plastic model for rheological data entry. Therefore, it becomes the preferred rheological model of blood and chocolate. Recently, Ramesh *et al* [6] analysed the steam of Casson liquid past an extending sheet with Catteneo-Christove heat diffusion. Ibrar *et al* [7] explicated the influence of thermal radiation on Casson fluid stream with suspension of nanoparticles through a thin needle. Hamid [8] deliberated the viscous-ohmic dissipative stream of Casson fluid past a thin needle with nanoparticles suspension. Kumar *et al* [9] explicated the Casson and Carreau nanofluid streams with porous medium. Khan *et al* [10] pondered the Casson liquid flow through a stretchy surface with radiation effect.

Brownian movement and thermophoresis are the methods of mass and heat transfer of small particle movements in the form of thermal decay and concentration gradients which affect the small particles associated with bulk surfaces. The thermophoresis and Brownian movements are important factors in heat and mass transfer problems. It is widely used in various fields such as nuclear safety systems, aerospace, hydrodynamics, aerosol technology, and air pollution. In recent days, several researchers deliberated the thermophoresis effect and Brownian movement on the liquid flow through diverse surfaces. Hussain and Ahmed [11] studied the flow of liquid through a porous enclosure by using Buongiorno's nanofluid model. Khan *et al* [12] scrutinized the Brownian motion and thermophoresis effects on nanoliquid stream through a microchannel with a radiation effect. Jayadevamurthy *et al* [13] explicated the bioconvective stream of hybrid nanofluid through a moving rotating disk by considering thermophoresis and Brownian motion effects. Khan *et al* [14] utilized Buongiorno's nanofluid model to deliberate the non-Newtonian liquid stream through stretchy surface. Hayat *et al* [15] explored the non-Newtonian liquid flow by using thermophoresis and Brownian motion effects.

The importance of radiation plays a vital role in many physical problems. Radiation is a heat transference process that distributes heat energy through fluid particles. The impact of radiation on the stream of liquids reflects a major characteristic of engineering and many industrial developments including high temperatures, such as the production of paper plates, freezing of metal fragments, the manufacture of electrical chips, and fuel pumps. Recently, Hussain [16] discussed the dissipative flow of fluid with radiation effect. Sheikholeslami *et al* [17] scrutinized the impact of thermal radiation on nanoliquid stream. Mehmood *et al* [18] expounded the radiative flow of nanoliquid by means of KKL-model. Khan *et al* [19] inspected the radiative stream of non-Newtonian liquid with nanoparticles suspension. Gowda *et al* [20] explicated the radiative stream of second grade nanofluid.

In many cases, it has been observed that there is a high concentration of extracellular species that can cause the impact of a blow. The idea of the impact of blowing comes from Stefan's problem. Stefan flow refers to the movement of the effects of chemical reactions from the scattering of species on the visual connector which can create a blowing effect. This explosion effect can occur in an inert position and is therefore completely different from the suction effect on the wall associated with the injection in open areas. The concept of wall injection is presented in the Stefan problem and was first investigated by Spalding [21]. Encouragement of the Stefan blowing constraint on a stream of nanofluid past a solid rotating stretchy disk was scrutinised by Latiff *et al* [22]. Amirsom *et al* [23] numerically explained the stimulation of Stefan blowing on the convective stream of nanoliquid past a thin needle with microorganisms. Alamri *et al* [24] schematically depicted the significance of Stefan blowing on the Poiseuille nanofluid flow over the parallel plates. Lund *et al* [25] reported a model for studying the impact of Stefan blowing on the Casson nanofluid stream in the occurrence of radiation effect.

The thermal-diffusion (Soret) effect is the mass transfer caused by a thermal gradient. The Diffusion thermo effect, also known as the Dufour effect, is the energy flux produced by a composition gradient. The Soret-Dufour effects are generally smaller in magnitude than the effects defined by Fourier's and Fick's rules, and they are often ignored in mass and heat transport phenomena. In addition, the Dufour and Soret effects in the presence of thermal radiation have practical uses in solar power technology, electrical power generation, high temperature systems, nuclear reactors, and many other fields. Recently, Hayat *et al* [26] deliberated the Dufour-Soret effects on radiative flow of second grade liquid above an elastic sheet. Khan *et al* [27] explicated the Dufour-Soret effects on convective flow of Carreau–Yasuda fluid. Imtiaz *et al* [28] expounded the Dufour-Soret effects on flow of viscous liquid past a curved elastic surface. Jawad *et al* [29] elucidated the radiative flow of liquid with Marangoni convection and Dufour-Soret effects.

Inspired by literature mentioned above, this study investigates the impact of non-linear thermal radiation on Casson liquid flow past a moving thin needle with Stefan blowing, Dufour, Soret, thermophoresis and Brownian motion effects. This model as practical applications in the development of novel surgical devices for cell conveyance to the central nervous system. Blood flow in the blood vessels is a communal example of Casson liquid stream among other innovative applications of this liquid model. Graphs are drawn for various parameters against velocity, temperature and concentrations gradients. Results are modified to limited cases to make reasonable study.

2. Governing equations and physical description

In this problem, we consider the model of steady flow and heat transfer analysis of Casson nanofluid over a moving thin needle with a constant velocity U_w in a parallel free stream as shown in figure 1. The influences of non-linear radiation along with Stefan blowing, Soret and Dufour effects are also invoked. Furthermore, the room temperature and the concentration of the needle are supposed to be fixed, such that $T_w > T_\infty$ and $C_w > C_\infty$. Further, the shape of the thin needle is specified by $r = R(x) = \sqrt{\frac{\nu c x}{U}}$ in which composite velocity $U = U_w + U_\infty \neq 0$. Flow is laminar and the slippage is ignored. The needle is considered thin when its thickness does not exceed that of the boundary layer over it. Since, the needle is assumed to be thin, it is also assumed that the effect of its transverse curvature is of importance but the pressure gradient along the body may be neglected.

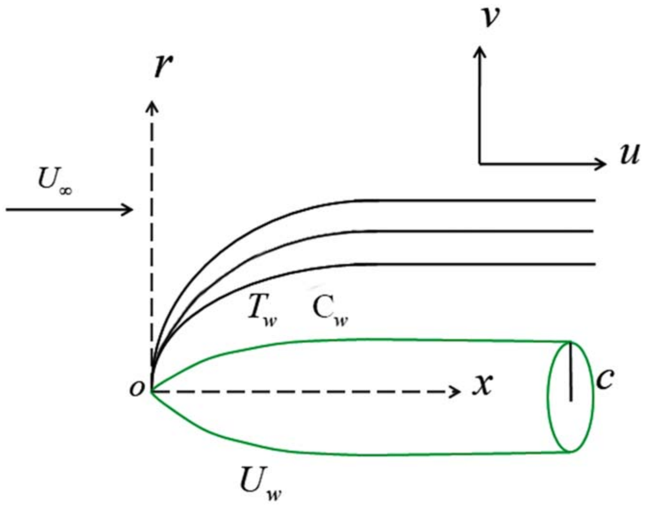

Figure 1. Flow geometry of the considered physical model.

The governing equations of the above assumed flow are given by ([30–32]):

$$\frac{\partial}{\partial x}(ru) + \frac{\partial}{\partial r}(rv) = 0, \tag{1}$$

$$u\frac{\partial u}{\partial x} + v\frac{\partial u}{\partial r} = \left(1 + \frac{1}{\beta^*}\right)\frac{\mu}{\rho}\frac{1}{r}\frac{\partial}{\partial r}\left(r\frac{\partial u}{\partial r}\right), \tag{2}$$

$$\begin{aligned} u\frac{\partial T}{\partial x} + v\frac{\partial T}{\partial r} &= \alpha\frac{1}{r}\frac{\partial}{\partial r}\left(r\frac{\partial T}{\partial r}\right) \\ &+ \tau\left(D_B\frac{\partial T}{\partial r}\frac{\partial C}{\partial r} + \frac{D_T}{T_\infty}\left(\frac{\partial T}{\partial r}\right)^2\right) \\ &+ \frac{1}{\rho C_p}\left[\begin{array}{c}\frac{16\sigma^* T^3}{3k^*}\frac{\partial^2 T}{\partial r^2} + \\ \frac{16\sigma^* 3T^2}{3k^*}\left(\frac{\partial T}{\partial r}\right)^2\end{array}\right] \\ &+ \frac{D_m K_T}{C_p C_s}\frac{1}{r}\frac{\partial}{\partial r}\left(r\frac{\partial C}{\partial r}\right), \end{aligned} \tag{3}$$

$$\begin{aligned} u\frac{\partial C}{\partial x} + v\frac{\partial C}{\partial r} &= D_B\frac{1}{r}\frac{\partial}{\partial r}\left(r\frac{\partial C}{\partial r}\right) \\ &+ \frac{D_T}{T_\infty}\frac{1}{r}\frac{\partial}{\partial r}\left(r\frac{\partial T}{\partial r}\right) + \frac{D_m K_T}{T_m}\frac{1}{r}\frac{\partial}{\partial r}\left(r\frac{\partial T}{\partial r}\right). \end{aligned} \tag{4}$$

The boundary constraints for the current study are as follow:

$$\begin{aligned} &u = U_w,\ v = -\frac{D_B}{1 - C_w}\left(\frac{\partial C}{\partial r}\right),\ T = T_w, \\ &C = C_w \text{ at } r = R(x), \end{aligned} \tag{5}$$

$$u = U_\infty,\ T \to T_\infty,\ C \to C_\infty \text{ as } r \to \infty. \tag{6}$$

Stream function and similarity variables for the developed governing equations are as follow:

$$\psi = \nu x f(\eta), \quad \eta = \frac{Ur^2}{\nu x}.$$

The velocity components $u = \frac{1}{r}\frac{\partial\psi}{\partial r}$ and $v = -\left(\frac{1}{r}\right)\frac{\partial\psi}{\partial x}$ are related to the physical stream function ψ according to, $u = 2Uf'(\eta)$, $v = -\frac{\nu}{r}[f(\eta) - \eta f'(\eta)]$. Further, $\frac{T - T_\infty}{(T_w - T_\infty)} = \theta(\eta)$, $\frac{C - C_\infty}{C_w - C_\infty} = \chi(\eta)$.

After implementation of the similarity variables, equation (1) is automatically satisfied and the remaining expressions are converted as:

$$\left(1 + \frac{1}{\beta^*}\right)2(\eta f''' + f'') + ff'' = 0, \tag{7}$$

$$\frac{2}{Pr}(\eta\theta'' + \theta') + f\theta' + 2\eta[N_b\theta'\chi' + N_t\theta'^2] + \frac{4}{3}\frac{1}{N_r Pr}[1 + \theta(\theta_r - 1)]^2\{(1 + (\theta_r - 1)\theta)(\theta' + 2\eta\theta'') + 6\eta(\theta_r - 1)\theta'^2\} + 2Du[\eta\chi'' + \chi'] = 0, \tag{8}$$

$$\frac{2}{Sc}[\eta\chi'' + \chi'] + f\chi' + \frac{2}{Sc}\frac{N_t}{N_b}[\eta\theta'' + \theta'] + 2Sr(\eta\theta'' + \theta') = 0. \tag{9}$$

Corresponding reduced boundary conditions are given by:

$$f'(c) = \frac{\lambda}{2}, f(c) = \frac{2c}{Sc}s\chi'(c) + c\frac{\lambda}{2}, \quad \theta(c) = 1, \chi(c) = 1, \tag{10}$$

$$f'(\infty) = \frac{1 - \lambda}{2}, \theta(\infty) = 0, \chi(\infty) = 0. \tag{11}$$

Where, $s < 0$ signifies mass suction and $s > 0$ signifies mass blowing as defined in [33].

Where, dimensionless parameters are defined as follows:

$$Pr = \frac{\nu}{\alpha}, Sc = \frac{\nu}{D_B}, N_t = \frac{\tau}{\nu}\frac{D_T}{T_\infty}(T_w - T_\infty),$$
$$N_b = \frac{\tau}{\nu}D_B(C_w - C_\infty), s = \frac{C_w - C_\infty}{1 - C_w}, N_r = \frac{k^*k_f}{4\sigma^* T_\infty^3},$$
$$Re_x = \frac{Ux}{\nu}, \theta_r = \frac{T_w}{T_\infty}, \lambda = \frac{U_w}{U},$$
$$Sr = \frac{D_m K_T(T_w - T_\infty)}{\nu T_m(C_w - C_\infty)}, Du = \frac{D_m K_T(C_w - C_\infty)}{\nu C_p C_s(T_w - T_\infty)}.$$

Mathematically, the surface drag force, rate of heat and mass transfer are given by:

$$\sqrt{Re_x}C_f = \left(1 + \frac{1}{\beta^*}\right)4\sqrt{c}f''(c), \tag{12}$$

$$\frac{1}{\sqrt{Re_x}}Nu = -2\sqrt{c}\theta'(c)\left[1 + \frac{4}{3N_r}(1 + (\theta_r - 1)\theta(c))^3\right], \tag{13}$$

$$\frac{1}{\sqrt{Re_x}}Sh_x = -2\sqrt{c}\chi'(c). \tag{14}$$

Table 1. The comparison of $f''(c)$ values for some reduced cases when $\lambda = 0$.

c	0.1	0.01	0.001
Souayeh *et al* [2]	1.288 801	8.492 412	62.163 71
Ishak *et al* [34]	1.2888	8.4924	62.1637
Chen and Smith [35]	1.288 81	8.492 44	62.163 72
Current results	1.2888	8.4924	62.1637

3. Numerical method

For various values of pertinent governing parameters, an efficient RKF-45 technique is employed to integrate the equations (7)–(9) along with the corresponding boundary constraints (10), (11). Initially, a two-point boundary value problem is reduced into first order differential equations. Also, to guess the missing initial conditions a shooting scheme is employed. Later, by using the RKF-45 method the resultant one is integrated. Here, the process uses a fourth- and a fifth-order Runge–Kutta scheme. The error of this algorithm can be found by subtracting these two values, and utilized for adaptive step sizing. The algorithm of the RKF-45 process is as follows:

$$k_0 = F(x_k, y_k),$$
$$k_1 = F\left(x_k + \frac{1}{4}h, y_k + \frac{h}{4}k_0\right),$$
$$k_2 = F\left(x_k + \frac{3}{8}h, y_k + h\left[\frac{3}{32}k_0 + \frac{9}{32}k_1\right]\right),$$
$$k_3 = F\left(x_k + \frac{12h}{13}, y_k + h\left(\frac{1932k_0}{2197} - \frac{7200k_1}{2197} + \frac{7296k_2}{2197}\right)\right),$$
$$k_4 = F\left(x_k + h, y_k + h\left[\frac{439k_0}{216} - 8k_1 + \frac{3680k_2}{513} - \frac{845}{4104}k_3\right]\right),$$
$$k_5 = F\left(x_k + \frac{h}{2}, y_k - \frac{8h}{27}k_0 + 2hk_1 - \frac{3544}{2565}hk_2 + \frac{1859}{4104}hk_3 - \frac{11}{40}hk_4\right).$$

$$y_{k+1} = y_k + \frac{25}{216}hk_0 + \frac{1408}{2565}hk_2 + \frac{2197}{4109}hk_3 - \frac{1}{5}hk_4,$$
$$y_{k+1} = y_k + \frac{16}{135}hk_0 + \frac{6656}{12825}hk_2 + \frac{28561}{56430}hk_3 - \frac{9}{50}hk_4 + \frac{2}{55}hk_5.$$

The value of η_∞ is chosen in such a way that the boundary conditions are asymptotically satisfied. The step size is selected as $\Delta\eta = 0.001$ with error tolerance to 10^{-6} is well-thought-out for convergence. Table 1 represents the comparative study

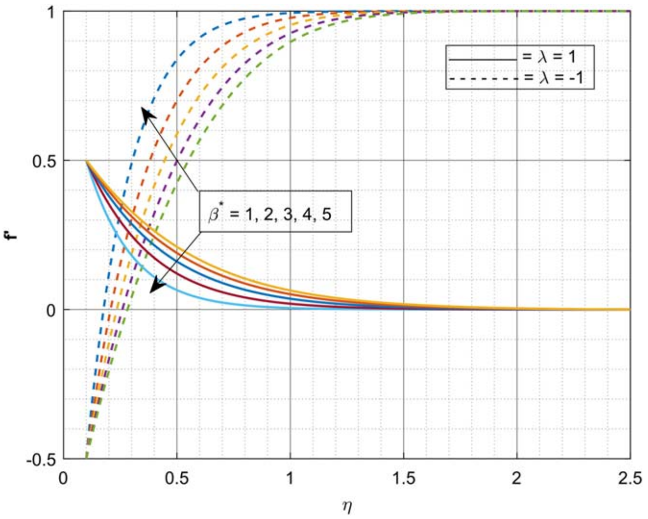

Figure 2. Domination of β^* on f'.

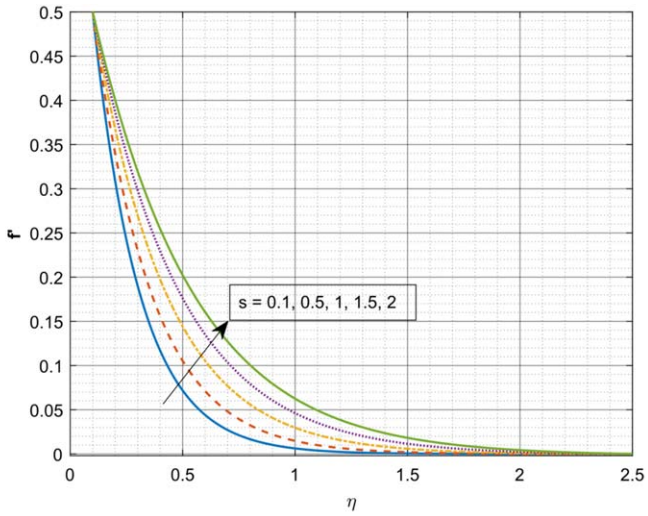

Figure 3. Domination of s on f'.

of existing works with present results and found a good agreement with each other.

4. Results and discussions

In this present examination, the non-linear thermal radiation impact on the stream of Casson fluid over a thin needle by means of Buongiorno's nanofluid model is discussed. At the boundary of the needle Stefan blowing effect is considered. The equations which govern the flow are converted to ODEs by choosing apt similarity variables. The impact of several dimensionless parameters like Casson parameter, heating parameter, radiative parameter, Schmidt number, Stefan blowing parameter, thermophoresis and Brownian motion parameters on concentration, thermal and velocity profiles are explicated graphically. Also, skin friction, rate of mass and heat transfer are deliberated graphically. Prandtl number has been specified to be adjusted for all of this while other parameters are set to be varied to assess their effects in terms of flow, heat and mass transfer.

Figure 2 portrays the domination of β^* on $f'(\eta)$ for the cases $\lambda = 1$ and $\lambda = -1$. Here, $\lambda = 1$ specifies the case of the moving needle in a sedentary ambient liquid and $\lambda = -1$ represents the free-streams wings in the negative x-direction. The escalating values of β^* declines the $f'(\eta)$ for the case $\lambda = 1$ while contrary movement is depicted in $f'(\eta)$ for the case $\lambda = -1$. Physically, a rise in values of β^* advances the liquid viscosity which results in declination of $f'(\eta)$. Figure 3 demonstrates the sway of s on $f'(\eta)$. An increase in s improves the $f'(\eta)$. We have detected that as the Stefan blowing parameter values upsurges, friction factor at the surface increases that is, week lateral mass flux into the boundary layer upsurges. The domination of N_b on $\theta(\eta)$ is revealed in figure 4. The growing values of N_b improves the $\theta(\eta)$. From a physical point of view, the growing value of N_b increases the thermal conductivity which automatically improves the thermal gradient. Figure 5 portrays the domination of N_t on $\theta(\eta)$. Here, inclination in N_t inclines the $\theta(\eta)$.

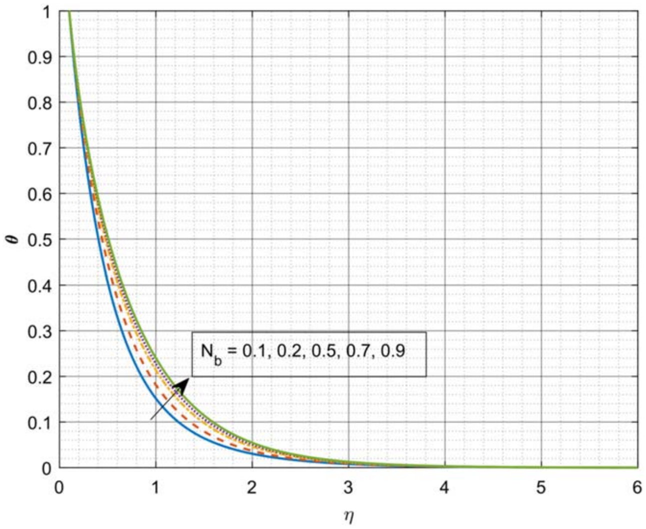

Figure 4. Domination of N_b on θ.

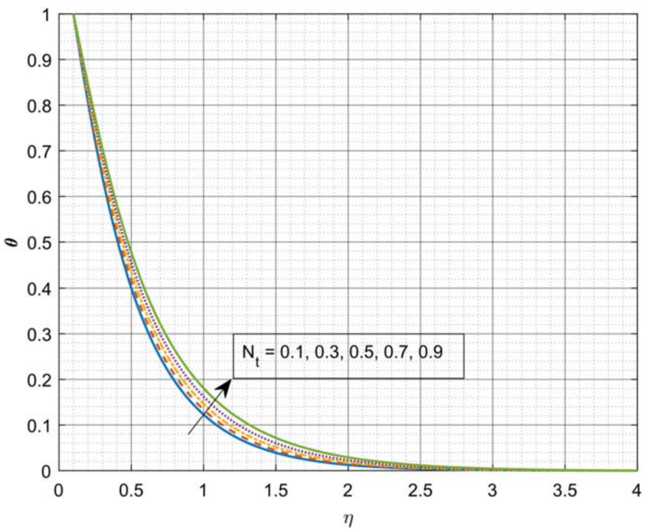

Figure 5. Domination of N_t on θ.

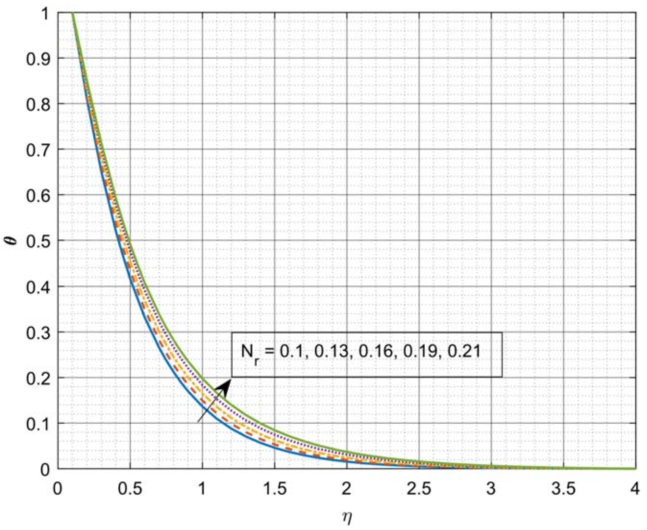

Figure 6. Domination of N_{r} on θ.

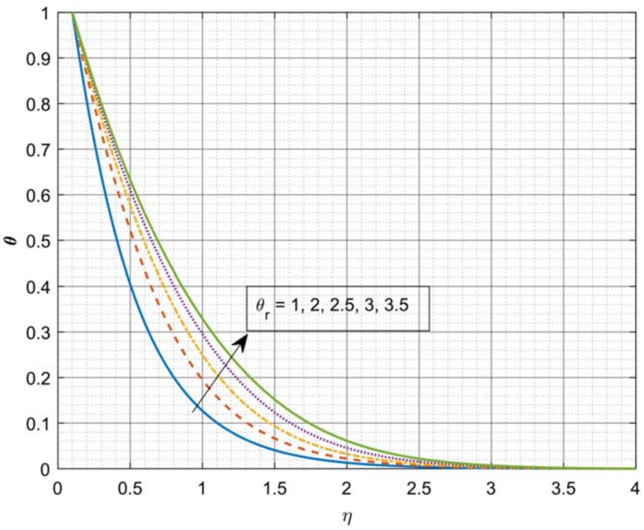

Figure 7. Domination of θ_{r} on θ.

Physically, for a warm surface ($N_t > 0$), thermophoresis impact improves the concentration of nanoparticles. Meanwhile, a hot needle fends off submicron particles which results in forming a particle-free layer near the surface. The encouragement of N_{r} on $\theta(\eta)$ is portrayed in figure 6. It is clear that, escalating values of N_{r} improves the thermal gradient. This is due to the physical fact that the inclination in N_{r} improves the thermal diffusivity which results in augmentation of $\theta(\eta)$. Figure 7 portrays the impact of θ_{r} on $\theta(\eta)$. The upsurge in θ_{r} improves the $\theta(\eta)$. Physically, the inclination in θ_r improves the inner temperature of liquid particles which results in augmentation of $\theta(\eta)$. Figure 8 illustrates the effect of Du over temperature profile. As the values of Du increases slightly, the thermal distribution increases. The thermal diffusion increases as Du increases which augments the temperature. Figure 9 explains the aspect of Sc on $\chi(\eta)$. The enhancing values of Sc weakens the $\chi(\eta)$. Physically, the upsurge in Schmidt number lessens the molecular diffusivity which results in decay of mass transfer. Figure 10 depicts the impact of Sr on $\chi(\eta)$. The upsurge in Sr improves the concentration gradient. Higher values of Sr reasons for low friction which in turn augments the $\chi(\eta)$. Figure 11 displays the impact of λ on skin friction versus Casson parameter. Here, the skin friction improves for the case $\lambda = 1$ but converse trend is depicted for the case $\lambda = -1$. The impact of radiative parameter on the heat transfer rate is showed in figure 12. The increase in N_{r} values decay the rate of heat transfer. The sway of Stefan blowing parameter on mass transfer rate is portrayed in figure 13. The gain in s deteriorates the rate of mass transfer

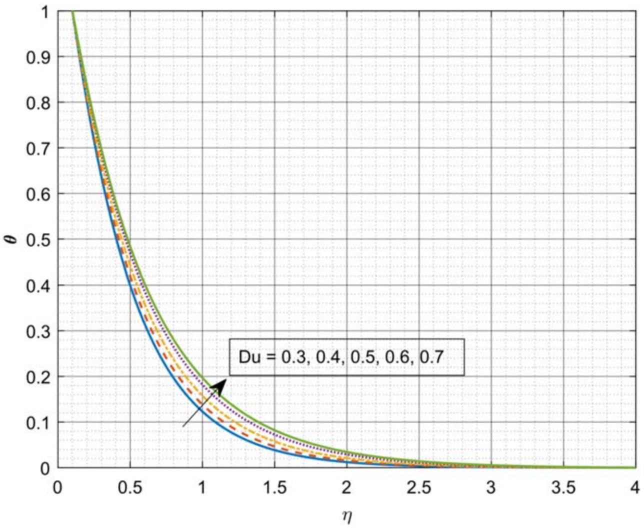

Figure 8. Domination of Du on θ.

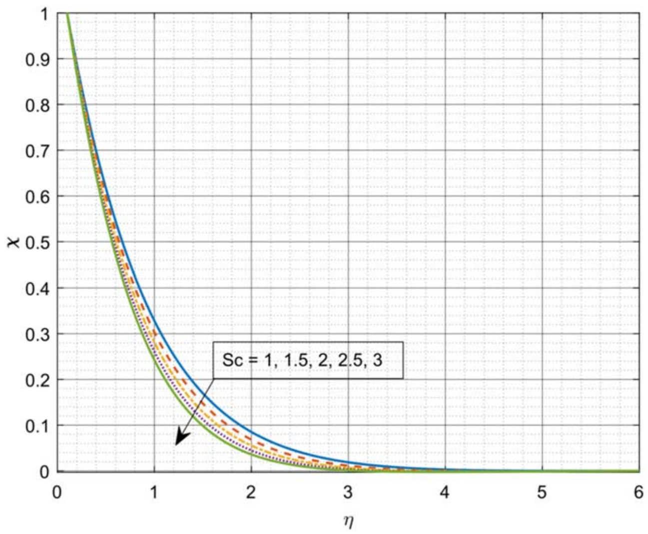

Figure 9. Domination of Sc on χ.

5. Conclusions

The present investigation explains the salient aspects of the incitement of non-linear thermal radiation on the Casson liquid stream over a moving thin needle with Stefan blowing, thermophoresis and Brownian motion effects. The influences

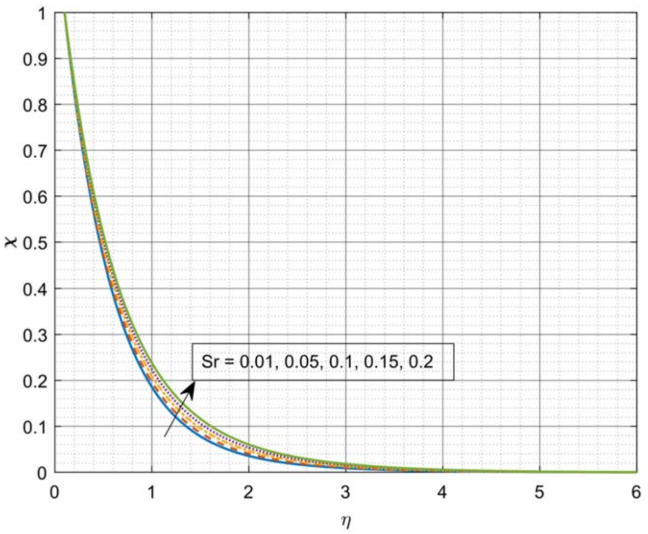

Figure 10. Domination of Sr on χ.

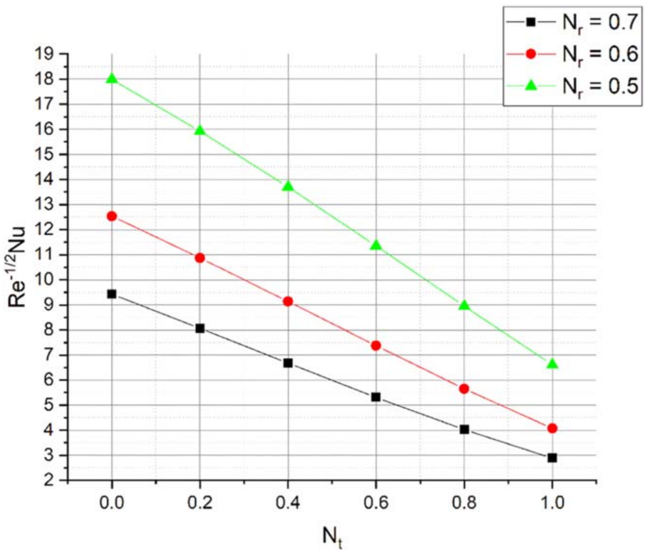

Figure 12. Domination of N_r on $Re_x{}^{1/2}Nu$.

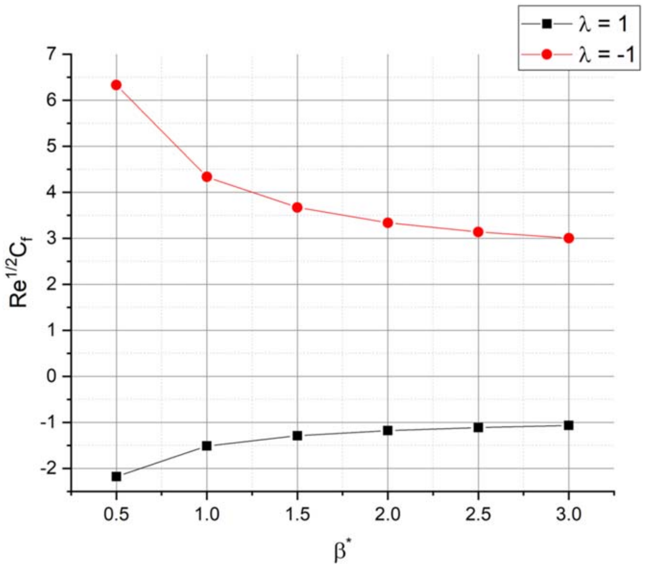

Figure 11. Domination of λ on $Re_x{}^{1/2}C_f$.

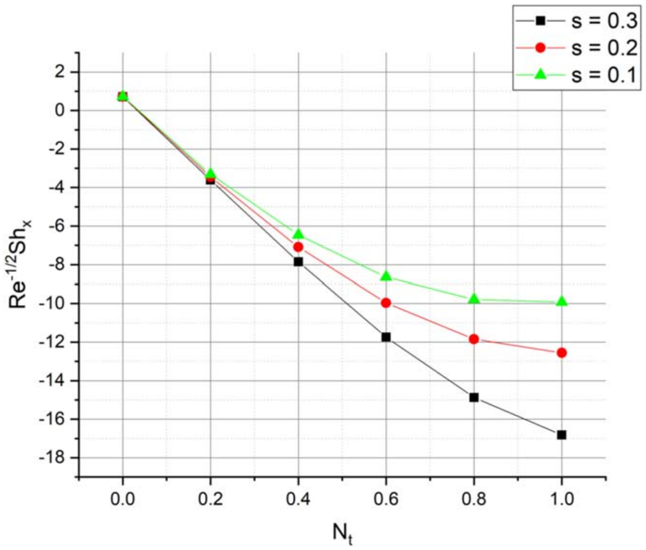

Figure 13. Domination of s on $Re_x{}^{1/2}Sh_x$.

of Dufour and Soret are also considered in the model. The impact of pertinent parameters on thermal, mass and velocity curves are deliberated graphically. The following conclusions are obtained from the present study:

- The growing values of N_b progresses the thermal gradient due to an increase in the thermal conductivity.
- The escalating values of N_r and θ_r improves the inner temperature of liquid particles resulting in an improvement in heat transfer.
- An upsurge in the Sc lessens the molecular diffusivity and it results in declination of mass transfer.
- The enhancing values of N_t improve the heat transfer.
- The thermal diffusion increases as Du increases which augments the temperature.
- Higher values of Sr reasons for low friction which in turn augments the mass transfer.

ORCID iDs

R Naveen Kumar https://orcid.org/0000-0002-0056-1452
R J Punith Gowda https://orcid.org/0000-0001-6923-6423
B C Prasannakumara https://orcid.org/0000-0003-1950-4666

References

[1] Mabood F, Nayak M K and Chamkha A J 2019 Heat transfer on the cross flow of micropolar fluids over a thin needle moving in a parallel stream influenced by binary chemical reaction and Arrhenius activation energy *Eur. Phys. J. Plus* **134** 427

[2] Souayeh B, Reddy M G, Sreenivasulu P, Poornima T, Rahimi-Gorji M and Alarifi I M 2019 Comparative analysis on non-linear radiative heat transfer on MHD Casson nanofluid past a thin needle *J. Mol. Liq.* **284** 163–74

[3] Ramesh G K, Shehzad S A and Izadi M 2020 Thermal transport of hybrid liquid over thin needle with heat sink/source and Darcy–Forchheimer porous medium aspects *Arab. J. Sci. Eng.* **45** 9569–78

[4] Xiong P-Y, Hamid A, Chu Y-M, Ijaz Khan M, Punith Gowda R J, Naveen Kumar R, Prasannakumara B C and Qayyum S 2021 Dynamics of multiple solutions of Darcy–Forchheimer saturated flow of Cross nanofluid by a vertical thin needle point *Eur. Phys. J. Plus* **136** 315

[5] Naveen Kumar R, Punith Gowda R J, Madhukesh J K, Prasannakumara B C and Ramesh G K 2021 Impact of thermophoretic particle deposition on heat and mass transfer across the dynamics of Casson fluid flow over a moving thin needle *Phys. Scr.* **96** 075210

[6] Ramesh G K, Gireesha B J, Shehzad S A and Abbasi F M 2017 Analysis of heat transfer phenomenon in magnetohydrodynamic casson fluid flow through Cattaneo–Christov heat diffusion theory *Commun. Theor. Phys.* **68** 91

[7] Ibrar N, Reddy M G, Shehzad S A, Sreenivasulu P and Poornima T 2020 Interaction of single and multi-walls carbon nanotubes in magnetized-nano Casson fluid over radiated horizontal needle *SN Appl. Sci.* **2** 677

[8] Hamid A 2020 Terrific effects of Ohmic-viscous dissipation on Casson nanofluid flow over a vertical thin needle: buoyancy assisting & opposing flow *J. Mater. Res. Technol.* **9** 11220–30

[9] Kumar R, Kumar R, Shehzad S A and Chamkha A J 2020 Optimal treatment of stratified Carreau and Casson nanofluids flows in Darcy-Forchheimer porous space over porous matrix *Appl. Math. Mech.* **41** 1651–70

[10] Khan M I, Khan M W A, Alsaedi A, Hayat T and Khan M I 2020 Entropy generation optimization in flow of non-Newtonian nanomaterial with binary chemical reaction and Arrhenius activation energy *Phys. Stat. Mech. Its Appl.* **538** 122806

[11] Hussain S and Ahmed S E 2019 Steady natural convection in open cavities filled with a porous medium utilizing Buongiorno's nanofluid model *Int. J. Mech. Sci.* **157–158** 692–702

[12] Khan A S *et al* 2020 Influence of interfacial electrokinetic on MHD radiative nanofluid flow in a permeable microchannel with Brownian motion and thermophoresis effects *Open Phys.* **18** 726–37

[13] Jayadevamurthy P G R, Rangaswamy N K, Prasannakumara B C and Nisar K S 2020 Emphasis on unsteady dynamics of bioconvective hybrid nanofluid flow over an upward–downward moving rotating disk *Numer. Methods Partial Differ. Equ.* (https://doi.org/10.1002/num.22680)

[14] Khan M I, Qayyum S, Nigar M, Chu Y-M and Kadry S 'Dynamics of Arrhenius activation energy in flow of Carreau fluid subject to Brownian motion diffusion *Numer. Methods Partial Differ. Equ.* n/a, no. n/a (https://doi.org/10.1002/num.22615)

[15] Hayat T, Khan S A, Ijaz Khan M, Momani S and Alsaedi A 2020 Cattaneo-Christov (CC) heat flux model for nanomaterial stagnation point flow of Oldroyd-B fluid *Comput. Methods Programs Biomed.* **187** 105247

[16] Hussain S 2017 Finite element solution for MHD flow of nanofluids with heat and mass transfer through a porous media with thermal radiation, viscous dissipation and chemical reaction effects *Adv. Appl. Math. Mech.* **9** 904–23

[17] Sheikholeslami M, Shehzad S A and Kumar R 2018 Natural convection of Fe_3O_4 -ethylene glycol nanouid under the impact of electric field in a porous enclosure *Commun. Theor. Phys.* **69** 667

[18] Mehmood K, Hussain S and Sagheer M 2017 Numerical simulation of MHD mixed convection in alumina–water nanofluid filled square porous cavity using KKL model: effects of non-linear thermal radiation and inclined magnetic field *J. Mol. Liq.* **238** 485–98

[19] Khan M I, Qayyum S, Waqas M, Hayat T and Alsaedi A 2020 Framing the novel aspects of irreversibilty in MHD flow of Williamson nanomaterial with thermal radiation near stagnation point *J. Therm. Anal. Calorim.* **139** 1291–9

[20] Punith Gowda R J, Naveen Kumar R, Jyothi A M, Prasannakumara B C and Sarris I E 2021 Impact of binary chemical reaction and activation energy on heat and mass transfer of marangoni driven boundary layer flow of a non-newtonian nanofluid *Processes* **9** 702

[21] Spalding D B 1954 Mass transfer in laminar flow *Proc. R. Soc. Lond. Ser. Math. Phys. Sci.* **221** 78–99

[22] Latiff N A, Uddin M J and Ismail A M 2016 Stefan blowing effect on bioconvective flow of nanofluid over a solid rotating stretchable disk *Propuls. Power Res.* **5** 267–78

[23] Amirsom N A, Uddin M J and Ismail A I M 2019 MHD boundary layer bionanoconvective non-Newtonian flow past a needle with Stefan blowing *Heat Transfer—Asian Res.* **48** 727–43

[24] Alamri S Z, Ellahi R, Shehzad N and Zeeshan A 2019 Convective radiative plane Poiseuille flow of nanofluid through porous medium with slip: an application of Stefan blowing *J. Mol. Liq.* **273** 292–304

[25] Ali Lund L, Omar Z, Raza J, Khan I and Sherif E-S M 2020 Effects of Stefan blowing and slip conditions on unsteady MHD casson nanofluid flow over an unsteady shrinking sheet: dual solutions *Symmetry* **12** 487

[26] Hayat T, Ullah I, Muhammad T and Alsaedi A 2017 Radiative three-dimensional flow with Soret and Dufour effects *Int. J. Mech. Sci.* **133** 829–37

[27] Ijaz Khan M, Hayat T, Afzal S, Imran Khan M and Alsaedi A 2020 Theoretical and numerical investigation of Carreau–Yasuda fluid flow subject to Soret and Dufour effects *Comput. Methods Programs Biomed.* **186** 105145

[28] Imtiaz M, Nazar H, Hayat T and Alsaedi A 2020 Soret and Dufour effects in the flow of viscous fluid by a curved stretching surface *Pramana* **94** 48

[29] Jawad M, Saeed A, Kumam P, Shah Z and Khan A 2021 Analysis of boundary layer MHD darcy-forchheimer radiative nanofluid flow with soret and dufour effects by means of marangoni convection *Case Stud. Therm. Eng.* **23** 100792

[30] Ahmad R, Mustafa M and Hina S 2017 Buongiorno's model for fluid flow around a moving thin needle in a flowing nanofluid: a numerical study *Chin. J. Phys.* **55** 1264–74

[31] Tuz Zohra F, Uddin M J, Basir M F and Ismail A I M 2020 Magnetohydrodynamic bio-nano-convective slip flow with Stefan blowing effects over a rotating disc *Proc. Inst. Mech. Eng. Part N J. Nanomater. Nanoeng. Nanosyst.* **234** 83–97

[32] Waleed Ahmed Khan M, Ijaz Khan M, Hayat T and Alsaedi A 2018 Entropy generation minimization (EGM) of nanofluid flow by a thin moving needle with nonlinear thermal radiation *Phys. B Condens. Matter* **534** 113–9

[33] Fang T and Jing W 2014 Flow, heat, and species transfer over a stretching plate considering coupled Stefan blowing effects from species transfer *Commun. Nonlinear Sci. Numer. Simul.* **19** 3086–97

[34] Ishak A, Nazar R and Pop I 2007 Boundary layer flow over a continuously moving thin needle in a parallel free stream *Chin. Phys. Lett.* **24** 2895

[35] Chen J L S and Smith T N 1978 Forced convection heat transfer from nonisothermal thin needles *J. Heat Transf.* **100** 358–62